Supporting Information

Ultrathin mesoporous graphitic carbon nitride nanosheets with functional cyano groups decoration and nitrogen vacancy defects for efficient selective CO_2 photoreduction

Junyi Li [a, b, ‡], Xiaohan Wang [a, ‡], Liang Huang [a], Liang Tian [a], Menny Shalom [b], Chunyan Xiong [c], Haijun Zhang [a, *], Quanli Jia[d], Shaowei Zhang [e], Feng Liang [a, *]

a The State Key Laboratory of Refractories and Metallurgy, Wuhan University of Science and Technology, Wuhan 430081, China

b Department of Chemistry and Ilse Katz Institute for Nanoscale Science and Technology, Ben-Gurion University of the Negev, Beer-Sheva 8410501, Israel

c School of Chemical Engineering and Pharmacy, Wuhan Institute of Technology, Wuhan 430074, China

d High Temperature Ceramic Institute, Zhengzhou University, Zhengzhou 450052, PR China

e College of Engineering, Mathematics and Physical Sciences, University of Exeter, Exeter Ex4 4QF, U.K.

* Corresponding author. Assoc. Prof. Feng Liang, E-mail: liangfengref@wust.edu.cn; Prof. Haijun Zhang, E-mail: zhanghaijun@wust.edu.cn, Tel: +86-27-68862829

‡ These authors contributed equally to this work.

Table S1 Textural parameters of nitrogen sorption analysis and elemental analysis for BCN and CNNS.

sample	S_{BET} (m^2/g)	Pore volume (cm^3/g)	Pore size (nm)	Elemental analysis (atom%)				
				C	N	H	O	C/N
BCN	7.0	0.63	5.25	34.1	49.9	13.7	1.1	0.68
CNNS	512.6	1.72	8.95	23.3	32.0	31.5	13.1	0.73

Table S2 Elemental compositions of BCN and CNNS based on XPS results.

	BCN		CNNS	
C (at.%)	**51.5%**	C-C (16.3%) C-NH_x(x=1, 2) (14.0%) C≡N (5.4 %) N=C-$(N)_2$ (64.3%)	**67.7%**	C-C (64.5%) C-NH_x (5.6%) C≡N (9.1%) N=C-$(N)_2$ (20.8%)
N (at.%)	**41.7%**	C=N-C (57.7%) N-$(C)_3$ (24.1%) N-H (18.2%)	**13.7%**	C=N-C (55.1%) C_3-N (26.1%) C≡N (11.6%) N-H (7.2%)
O (at.%)	**6.8%**	H_2O (88.9%) O_2 (11.1%)	**18.6%**	H_2O (46.6%) O_2 (53.4%)

Table S3 Comparison of photocatalytic CO_2 reduction performance of various materials.

Photocatalysts	**Conditions**	**Rate ($\mu mol \cdot g^{-1} \cdot h^{-1}$)**	**References**	**Year**
CNNS	H_2O, Xe lamp, 5 h ($\lambda \geq$ 200 nm/$\lambda \geq$ 420 nm)	CH_4: 50.8/23.0, CO: 5.1/1.9	This work	
BCN	H_2O, Xe lamp, 5 h ($\lambda \geq$ 200 nm/$\lambda \geq$ 420 nm)	CO: 2.6/1.1	This work	
N-CQDs-TiO_2	H_2O, Xe lamp, 6 h	CH_4: 3.98, CO: 6.13	[S1]	2018
g-C_3N_4	H_2O, Xe lamp, 5 h ($\lambda >$ 200 nm)	CH_4: 0.24, CO: 2.1	[S2]	2016
P-doped g-C_3N_4	H_2O, Vis ($\lambda \geq$ 420 nm), 4 h	CO: 2.37, CH_4: 1.81	[S3]	2018
Co_3O_4/CNS	H_2O, Xe lamp, 4 h	CO: 13.31, CH_4: 3.17	[S4]	2020
WO_3/g-C_3N_4	H_2O, UV (254$\leq \lambda <$ 420 nm)/Vis ($\lambda \geq$420 nm), 4 h	CO: 14.60/1.37, CH_4: 10.37/0.75	[S5]	2020
$Bi_4O_5Br_2$	H_2O, Xe lamp, 2 h	CO: 3.16, CH_4: 0.5	[S6]	2019
Ru/g-C_3N_4	H_2O, Xe lamp, 4 h (420$\leq \lambda <$780 nm)	CO: (4.78), CH_4: (0.78)	[S7]	2018

SnS_2/g-C_3N_4	H_2O, Xe lamp, 4 h (λ> 420 nm)	CH_4: 0.64, CH_3OH: 2.3	[S8]	2017
PdO/TiO_2	H_2O, UV light, 2 h	CO: 0.12, CH_4: 13.99	[S9]	2019
O-doped g-C_3N_4	H_2O, Xe lamp (λ> 420 nm)	CH_3OH: 0.88	[S10]	2017
MnO_2/g-C_3N_4	H_2O, Xe lamp, 6 h	CO: 3.4	[S11]	2017
NiO/g-C_3N_4	H_2O, Xe lamp, 8 h	CO: 4.17	[S12]	2018
Pt@Bi-TiO_2	H_2O, Hg lamp, 10 h	CH_4: 2.06	[S13]	2020
Au/C_3N_4	H_2O, Xe lamp, 2 h	CO：6.59, CH_4：1.55	[S14]	2018
Bi_2MoO_6	H_2O, Xe lamp, 6 h	CO：3.62	[S15]	2019
Ni-Bi co-doped TiO_2	H_2O, 250W Hg lamp, 10 h	CH_4：2.11	[S16]	2020

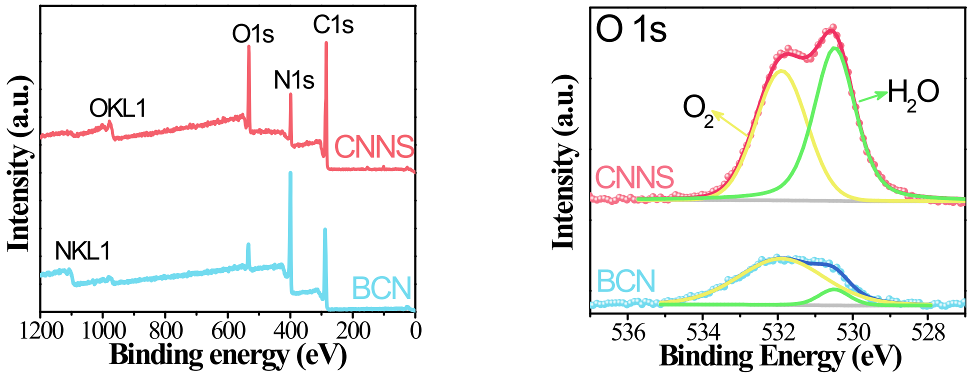

Figure S1 XPS wide spectra and high resolution O 1s XPS spectra of BCN and CNNS.

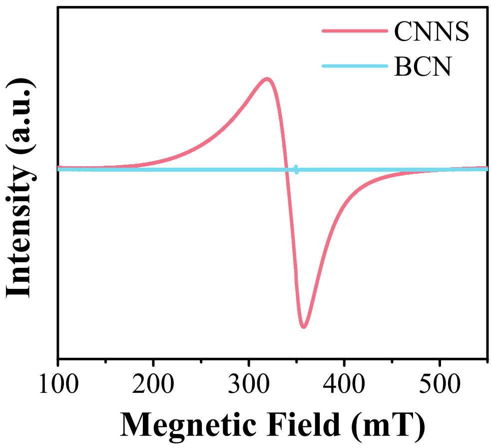

Figure S2 EPR spectra of BCN and CNNS.

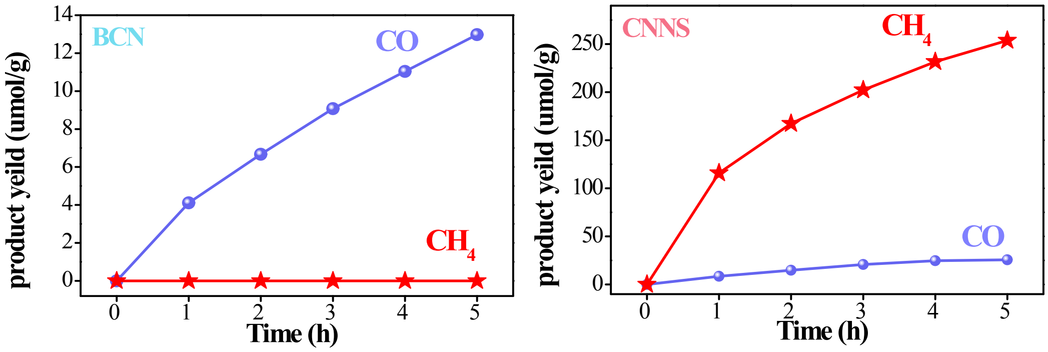

Figure S3. Time-production plots of the CO and CH_4 generated form the photocatalytic CO_2 reduction over the BCN (left) and CNNS (right). (photocatalysis condition: 0.05 g photocatalysts, 5 mL H_2O, Light $\lambda \geq 200$ nm, 20°C)

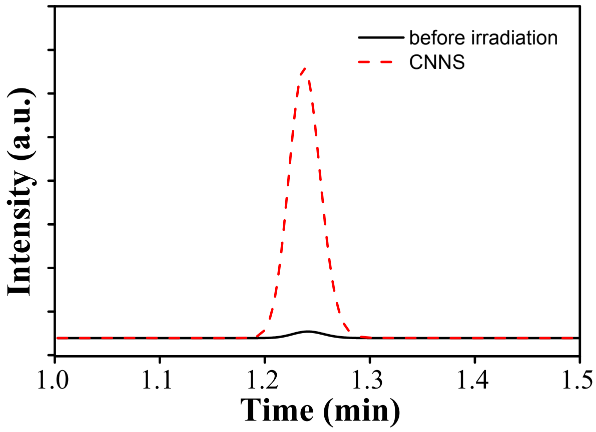

Figure S4. The GC spectra of resulting O_2 after photocatalytic CO_2-reduction reactions (visible-light-driven, λ≥420 nm) over CNNS.

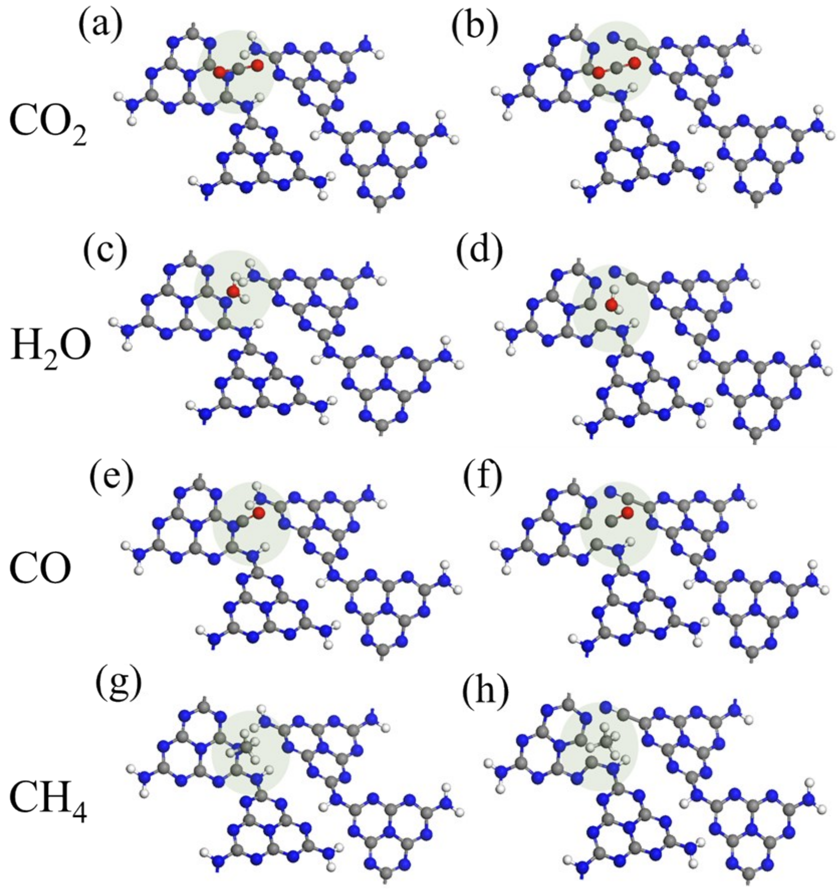

Figure S5 CO_2, H_2O, CO, CH_4 adsorption geometry on BCN (a, c, e, and g) and CNNS with nitrogen vacancy and cyano group (b, d, f, and h).

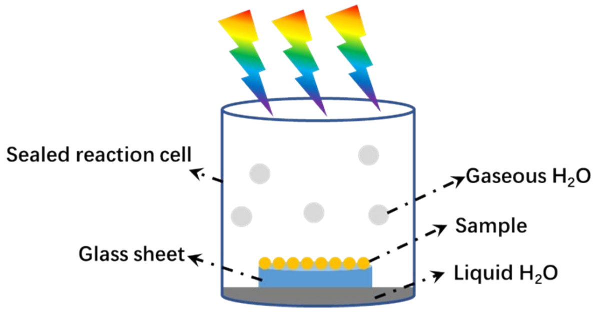

Figure S6 Illustration of the experimental setup for photocatalytic CO_2 reduction.

References

[S1]Li M, Wang M, Zhu L, et al. Facile microwave assisted synthesis of N-rich carbon quantum dots/dual-phase TiO_2 heterostructured nanocomposites with high activity in CO_2photoreduction[J]. Applied Catalysis B: Environmental, 2018, 231: 269-276.

[S2]Wang H, Sun Z, Li Q, et al. Surprisingly advanced CO_2 photocatalytic conversion over thiourea derived g-C_3N_4 with water vapor while introducing 200–420 nm UV light[J]. Journal of CO2 Utilization, 2016, 14: 143-151.

[S3]Li M, Zhang L, Fan X, et al. Core-shell $LaPO_4$/g-C_3N_4 nanowires for highly active and selective CO_2 reduction[J]. Applied Catalysis B: Environmental, 2017, 201: 629-635.

[S4]Hangfan Ma X L, Shiying Fan , Zhifan Yin , Guoqiang Gan , Meichun Qin , Penglei Wang , Yaxuan Li , Lianzhou Wang In Situ Formation of Interfacial Defects between Co-Based SpinelCarbon Nitride Hybrids for Efficient CO_2 Photoreduction[J]. ACS Applied Energy Materials, 2020, 3(5): 5083–5094.

[S5]Li X, Song X, Ma C, et al. Direct Z-Scheme WO_3/Graphitic Carbon Nitride Nanocomposites for the Photoreduction of CO_2[J]. ACS Applied Nano Materials, 2020, 3(2): 1298-1306.

[S6]Jin X, Lv C, Zhou X, et al. A bismuth rich hollow $Bi_4O_5Br_2$ photocatalyst enables dramatic CO_2 reduction activity[J]. Nano Energy, 2019, 64: 103955.

[S7]Ye F, Wang F, Meng C, et al. Crystalline phase engineering on cocatalysts: A promising approach to enhancement on photocatalytic conversion of carbon dioxide to fuels[J]. Applied Catalysis B: Environmental, 2018, 230: 145-153.

[S8]Di T, Zhu B, Cheng B, et al. A direct Z-scheme g-C_3N_4/SnS_2 photocatalyst with superior visible-light CO_2 reduction performance[J]. Journal of Catalysis, 2017, 352: 532-541.

[S9]Mekasuwandumrong O, Jantarasorn N, Panpranot J, et al. Synthesis of Cu/TiO_2 catalysts by reactive magnetron sputtering deposition and its application for photocatalytic reduction of CO_2 and H_2O to CH_4[J]. Ceramics International, 2019, 45(17): 22961-22971.

[S10] Fu J, Zhu B, Jiang C, et al. Hierarchical Porous O-Doped g-C_3N_4 with Enhanced Photocatalytic CO_2 Reduction Activity[J]. Small, 2017, 13(15).

[S11] Wang M, Shen M, Zhang L, et al. 2D-2D MnO_2/g-C_3N_4 heterojunction photocatalyst: In-situ synthesis and enhanced 2 reduction activity[J]. Carbon, 2017, 120: 23-31.

[S12] Tang J-y, Guo R-t, Zhou W-g, et al. Ball-flower like NiO/g-C_3N_4 heterojunction for efficient visible light photocatalytic CO_2 reduction[J]. Applied Catalysis B: Environmental, 2018, 237: 802-810.

[S13] Mohsen Moradi F K, Afsanehsadat Larimi Pt nanoparticles decorated Bi-doped TiO_2 as an efficient photocatalyst for CO_2 photo-reduction into CH_4[J]. Solar Energy, 2020, 211: 100-110.

[S14] Li H, Gao Y, Xiong Z, et al. Enhanced selective photocatalytic reduction of CO_2 to CH_4 over plasmonic Au modified g-C_3N_4 photocatalyst under UV–vis light irradiation[J]. Applied Surface Science, 2018, 439: 552-559.

[S15] Jun Di X Z, Cheng Lian, Mengxia Ji, Jiexiang Xia, Jun Xiong, Wu Zhou, Xingzhong Cao, Yuanbin She, Honglai Liu, Kian Ping Loh, Stephen J. Pennycook, Huaming Li, Zheng Liu. Atomically-thin Bi_2MoO_6 nanosheets with vacancy pairs for improved photocatalytic CO_2 reduction[J]. Nano Energy, 2019, 61: 54-59.

[S16] Nematollahi R, Ghotbi C, Khorasheh F, et al. Ni-Bi co-doped TiO_2 as highly visible light response nano-photocatalyst for CO_2 photo-reduction in a batch photo-reactor[J]. Journal of CO_2 Utilization, 2020, 41.